American Mineralogist, Volume 70, pages 65–73, 1985

An oxygen buffer for some peraluminous granites and metamorphic rocks

E-AN ZEN

U.S. Geological Survey
959 National Center, Reston, Virginia 22092

Abstract

The mineral assemblage biotite–garnet–muscovite–magnetite–quartz and its subsets are common in many peraluminous granites, schists, and gneisses. If the biotite and garnet are reasonably iron rich, then the system is a useful buffer for oxygen fugacity. Available thermochemical data indicate that, in temperature–oxygen fugacity space, the buffer curve is located between the hematite–magnetite curve and the quartz–magnetite–fayalite curve, in a region that previously had no buffer curve applicable to peraluminous rocks. The buffer equation, partially taking into account the departures of biotite, garnet, and muscovite compositions from their end-member formulae, is:

$$\log f_{O_2} = 10.29 - 26284T^{-1} + 0.148(P-1)T^{-1} - 4\log X_{Si}^{bt} - 3\log X_{Fe^{2+}}^{bt} - 3\log X_{Fe^{2+}}^{gt} + 2\log X_{Al}^{muvi} + 4\log X_{Si}^{mu} \pm (1 + 650/T)$$

Examples of applications are given for three peraluminous granitic rocks and three pelitic schists. The calculated oxygen fugacity values, corrected for mineral compositions, generally agree with published estimated values based on the compositions of coexisting iron and titanium oxide phases.

Introduction

If hydrogen can diffuse into and out of a system in which a redox reaction is possible, then the fugacity of oxygen at a given temperature and total pressure must be regarded as a boundary-value variable, and its value will be independent of the fugacity of H_2O. Various mineralogical means have been proposed to estimate the oxygen fugacity, particularly for magmatic systems (e.g., Wones, 1966, 1981; Czamanske and Wones, 1973). I propose another oxygen buffer system, involving the mineral assemblage annite-rich biotite (B), almandine-rich garnet (A), muscovite (M), magnetite (M), and quartz, hereafter referred to as the BAMM buffer system. This system is useful for many peraluminous granites, schists and gneisses. This paper presents the thermochemical calculations, estimates the uncertainties in the data, and considers some petrologic applications.

Thermochemical data

Sources of data

The sources of thermochemical data used in the calculations are summarized in Table 1. In addition to the phases involved in the BAMM reaction, the data for high sanidine are included because they were used to calculate the data for annite.

The temperature-dependent Gibbs free energy data for almandine are from a recent compilation by Larry Anovitz and J. L. Haas, Jr. (1983, written communication) for stoichiometric almandine, $Fe_3Al_2Si_3O_{12}$. The same, mutually consistent data source was used for stoichiometric magnetite, Fe_3O_4. At 298 K and 1 bar, the Gibbs free energy for magnetite is about 1.5 kJ more negative than that tabulated by Robie et al. (1978).

The temperature-dependent Gibbs free energy data for high sanidine, $KAlSi_3O_8$, are from Robie et al. (1978). The same data source was used for stoichiometric $2M_1$ muscovite, $KAl_2AlSi_3O_{12}H_2$, and for quartz, SiO_2.

The data for annite require extensive comment. The values in Table 1 are for the stoichiometric and fully hydroxylated, ferric-iron free annite, $KFe_3^{2+}AlSi_3O_{12}H_2$. Helgeson et al. (1978) calculated a set of thermochemical parameters for a phase of this composition. Zen (1973) calculated the thermochemical data for an oxyannite having ten percent of the iron in the ferric state, and a corresponding deficiency in hydrogen. Both sets of calculations were based on the hydrogen-buffered hydrothermal studies of Wones et al. (1971) for the breakdown of oxyannite of variable ferric–ferrous ratios to high sanidine and magnetite.

Hewitt and Wones (1981) corrected the data of Wones et al. (1971). Partin et al. (1983) further improved the equation for the breakdown of annite of variable ferric iron content as given by Hewitt and Wones (1981). Partin et al. (1983) directly determined the ferric/ferrous ratios

0003–004X/85/0102–0065$02.00

Table 1. Thermodynamic data used for calculating the BAMM buffer equilibria.

Property / Phase	G°(298, 1)	S°_f (T)	V	Reference
Annite $KFe_3AlSi_3O_{12}H_2$	-4,808.86 kJ ± 10.8 kJ	From Third Law entropy and Cp data, converted to S_f at intervals of 100K	154.30 ± 0.44 cm^3	G: This study S: Helgeson and others, 1978 V: Robie and others, 1967
Almandine $Fe_3Al_2Si_3O_{12}$	-4,942.704 kJ ± 1.54 kJ	Data given as f(T) at intervals of 100K	115.27 ± 0.04 cm^3	G: Larry Anovitz and J.L. Haas, Jr., 1983 written commun. S: Same V: Robie and others, 1967
Muscovite $KAl_2AlSi_3O_{12}H_2$	-5,600.671 kJ ± 3.3 kJ	Data given as f(T) at intervals of 100K	140.71 ± 0.18 cm^3	G: Robie and others, 1978 S: Same V: Robie and others, 1967
Sanidine $KAlSi_3O_8$	-3,739.776 kJ ± 3.4 kJ	Data given as f(T) at intervals of 100K	109.05 ± 0.10 cm^3	G: Robie and others, 1978 S: Same V: Robie and others, 1967
Magnetite Fe_3O_4	-1,014.135 kJ ± 2 kJ	Data given as f(T) at intervals of 100K	44.524 ± 0.008 cm^3	G: Larry Anovitz and J.L. Haas, Jr., 1983, written commun.; uncertainty from Robie and others, 1978 S: Anovitz and Haas, same V: Robie and others, 1967
Quartz SiO_2	-856.288 kJ ± 1.1 kJ	Data given as f(T) at intervals of 100K	22.688 ± 0.001 cm^3	G: Robie and others, 1978 S: Same V: Robie and others, 1967

of synthetic annite as a function of the equilibrium temperature (*Te*), equilibrium total pressure (*Pe*), and oxygen fugacity, fO_2, and thereby extrapolated the data to end member annite. David A. Hewitt (1983, written communication) very generously provided me with a prepublication copy of the equation for this extrapolated equilibrium, consistent with the data of Partin et al. (1983), but slightly different from the equation of Hewitt and Wones (1981):

$$\log[f_{H_2}/X^3_{Fe^{2+}}X^2_{OH}] = 8.58 - 6758T^{-1} + 0.0042(P - 1)T^{-1} \quad (1)$$

where f_{H_2} is the fugacity of H_2, $X_{Fe^{2+}}$ is the mole fraction of ferrous iron in the octahedral site, i.e., Fe^{2+}(vi)/3, in the biotite, and X_{OH} is the mole fraction of OH in the hydroxyl position in the biotite. Equation (1) is used to calculate the Gibbs free energy of end member annite (simply referred to as "annite" hereafter) from the reaction

$$\underset{\text{annite, ann}}{KFe_3AlSi_3O_{12}H_2} = \underset{\text{sanidine, san}}{KAlSi_3O_8} + \underset{\text{magnetite, mt}}{Fe_3O_4} + H_2 \quad (2)$$

The Gibbs free energy of annite can be obtained by using the following relation:

$$G^\circ_{ann}(298.15, 1) = \int_{298.15}^{Te} S^\circ_{f,ann}(T)dT + G^\circ_{san}(Te,1) + G^\circ_{mt}(Te,1) + \Delta V_s(Pe - 1) + G^\circ_{H_2}(Te,f) \quad (3)$$

where G° is the Gibbs free energy of formation of the phase from the elements at the specified T and P. S°_f is the entropy of formation of the phase from the elements, at T and 1 bar, and $\Delta V_s = V_{san} + V_{mt} - V_{ann}$.

To calculate G°_{ann}, I set the fugacity of hydrogen at unity, so that for end member annite the left hand side of equation (1) becomes zero, and the equilibrium temperature, *Te*, for the reaction of equation (2) can be calculated explicitly as a function of *Pe*. Four values of *Pe*, the total pressure, were used: 1 bar, and 1, 2, and 3 kbar. The corresponding values of *Te* are 787.7, 787.2, 786.7, and 786.2 K; these define the stability of end member annite at f_{H_2} of unity.

The closely-spaced *Te* values do not allow estimation of the entropy of formation of annite by difference (Zen, 1973), so I adopted the estimation of Helgeson and others (1978) for an annite having ordered tetrahedral Al and Si atoms: $S(298.15, 1) = 398.31\ JM^{-1}K^{-1}$; $C_p = 445.30 + 124.56 \times 10^{-3}T - 80.79 \times 10^5T^{-2}\ JM^{-1}K^{-1}$. Using these values and the data listed in Table 1, I obtained G°_{ann} (298.15, 1) from the four pairs of *T*, *P* values given above ($G^\circ_{H_2} = 0$ because $f_{H_2} = 1$). These values are, in order of 1 bar, and 1, 2, and 3 kbar, −4,808,837; −4,808,850; −4,808,863; and −4,808,876 JM^{-1}; the mean value is −4,808,857 JM^{-1}. This value, based on the stability data of Partin et al. (1983), is about 150 joules less negative than would be obtained using the stability data of Hewitt and Wones (1981) but is significantly more negative (annite more stable) than the value of −4,799.70 kJM^{-1}

calculated by Helgeson and others (1978) based on Wones and others (1971).

Robinson and Haas (1983) suggested a method to compute the entropy of a mineral from its chemical formula and cation coordinations. Using this method, the Third Law entropy of end member annite at 298.15 K and 1 bar is calculated to be 402.1 $JM^{-1}K^{-1}$; the temperature dependence of the entropy value is also slightly greater than that of Helgeson and others. The value of $G°$(298.15, 1) for end member annite is $-4{,}806.49$ kJM^{-1}. However, these minor changes do not affect the location of the calculated BAMM buffer curve by more than 0.1 log fO_2 units at temperatures greater than 600 K.

If the tetrahedral Al and Si are completely and ideally disordered, the entropy would be 18.70 $JM^{-1}K^{-1}$ higher than Helgeson's value, and the calculated $G°_{ann}$ (298.15, 1) would be $-4{,}799.72$ kJM^{-1}. By coincidence this is nearly identical to the value of Helgeson and others (1978), but the temperature dependence of $G°_{ann}$ is greater for disordered annite. The two sets of $G°_{ann}$ coincide in value at about 788 K, the reference temperature of my thermochemical calculations.

Calculation of the BAMM buffer equilibrium curve

As a first approximation in the calculations, I used the end member formulae for all the phases of the BAMM reaction. The reaction can be written as

$$\underset{\text{annite, ann}}{KFe_3AlSi_3O_{12}H_2} + \underset{\text{almandine, alm}}{Fe_3Al_2Si_3O_{12}} + O_2$$

$$= \underset{\text{muscovite, mu}}{KAl_2AlSi_3O_{12}H_2} + \underset{\text{magnetite, mt}}{2\,Fe_3O_4} + \underset{\text{quartz, q}}{3\,SiO_2} \qquad (3)$$

At equilibrium, the oxygen fugacity is given by

$$2.303\,RT \log fO_2 = \Delta G_s\,(Te, 1) + \Delta V_s\,(Pe - 1) \qquad (4)$$

where $\Delta G_s(Te,1) = G_{mu}(Te,1) + 2G_{mt}(Te,1) + 3G_q(Te,1) - G_{ann}(Te,1) - G_{alm}(Te,1)$ and ΔV_s is similarly defined. The value of ΔV_s for the reaction, $+28.252$ cm^3, is large compared to the volume changes for common buffer oxide reactions (see Huebner, 1971), so the BAMM buffer system is relatively sensitive to pressure; the more reduced side is favored by higher pressure.

Using the data of Table 1, I evaluated equation (4) at intervals of 100 degrees centigrade; the results were then fitted to a least-squares equation that related log fO_2 to T^{-1}. The equation applicable to the end member phases is

$$\log fO_2 = 10.29 - 26284T^{-1} + 0.148(P - 1)T^{-1} \pm 650/T \qquad (5)$$

The basis for the error estimation is given in a later section of this paper. The result is plotted for 1 bar and 4 kbar pressures in Figure 1. Equation (5) will be referred to hereafter as the "reference BAMM" buffer curve. For comparison, Figure 1 also shows the 1 bar and 4 kbar curves for three common reference buffers: quartz–magnetite–fayalite (QMF), nickel–bunsenite (NB), and hematite–magnetite (HM). Data for QMF are taken from Hewitt (1978); those for NB and HM are from Schwab and Küstner (1981) with the pressure term taken from Huebner (1971). The QMF curve is significantly more oxidizing than that given by Huebner (1971); the NB curve is nearly identical to Huebner's compiled value and the HM curve is slightly more reducing than Huebner's value.

Figure 1 shows that the reference BAMM buffer system is between the QMF buffer curve and the NB curve. At temperatures lower than 440°C, the reference BAMM curve appears to be slightly more reducing than QMF. The difference is small and is entirely within the range of uncertainties (see section on errors), nevertheless the data, taken at face value, are not consistent because the assemblage that involves muscovite, magnetite and quartz on one side (BAMM) must be less stable than the assemblage that involves only magnetite and quartz (QMF) on the same side.

Compositional corrections to the reference BAMM system

Several compositional corrections must be introduced for the practical use of the BAMM buffer system. Natural biotite is a complex solid solution, but the principal trends of solution are from annite toward phlogopite, $KMg_3AlSi_3O_{12}H_2$, and toward oxyannite, and also involve excess aluminum in both tetrahedral and octahedral sites. The correction for the activity of annite in the phlogopite–annite solid solution can be expressed by the ideal three-site model for octahedral substitution (Mueller, 1972; Wones, 1972, Holdaway, 1980):

$$\Delta G_{ann} = +3RT \ln X^{bt}_{Fe^{2+}}.$$

The superscript bt identifies the phase as biotite. The effect of oxyannite is expressed in changing the value of $X_{Fe^{2+}}$ and in changing the value of X_{OH}, as indicated in equation (1).

Holdaway (1980) discussed the effect of excess Al on the thermodynamic properties of biotite. In natural biotite, the excess Al must be assigned to both the tetrahedral site and to the octahedral site; at least in part these substitutions can be described as a coupled substitution, $(Al^{iv}Al^{vi}) = (Fe^{2+,vi}Si^{iv})$. The effect of excess tetrahedral Al on the activity of end member annite can be computed in a straightforward manner; it is the difference in the Gibbs free energy correction due to the actual number of tetrahedral Al, Y, less the correction due to one atom of Al (end member annite), per 11-oxygen formula. Writing this difference in terms of the complementary Si atom distribution, we have

$$\Delta \ln fO_2 = 4 \ln [(4 - Y)/4] - 4 \ln [3/4] = 4 \ln (4 - Y)/3$$
$$= 4 \ln X^{bt}_{Si}$$

where X^{bt}_{Si} is defined as $(4 - Y)/3$.

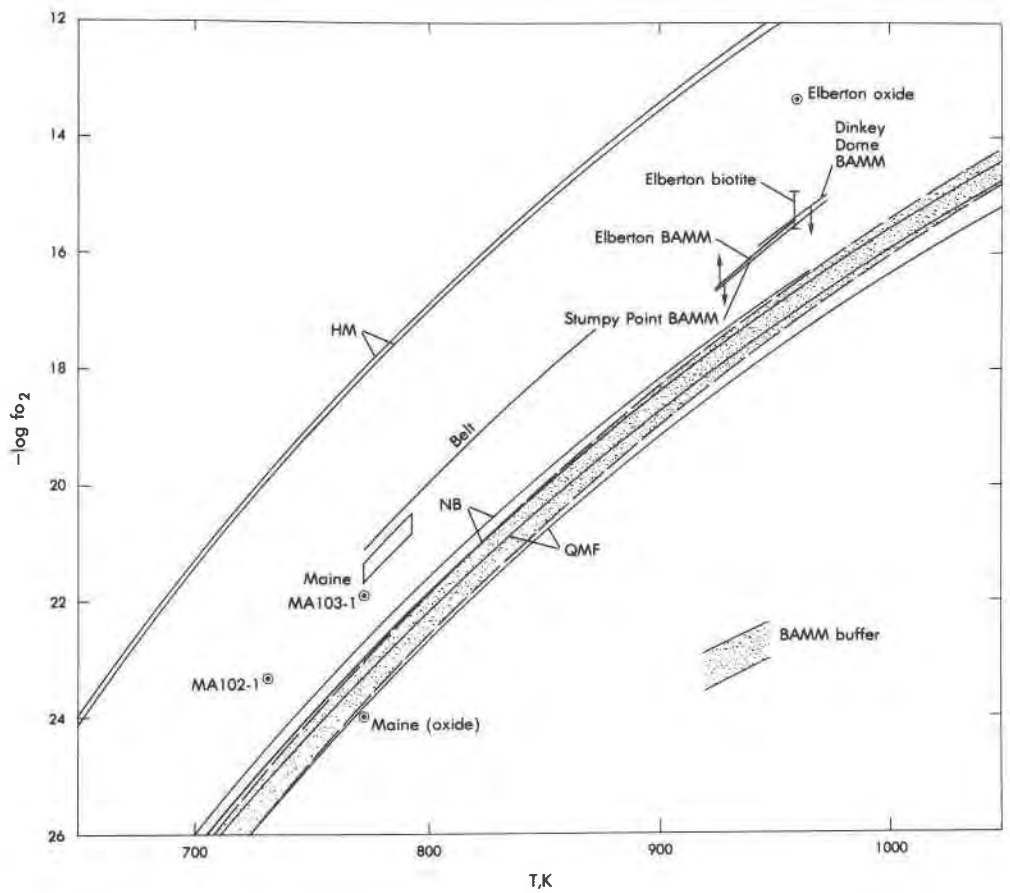

Fig. 1. The BAMM buffer curve, for 1 bar pressure and 4 kbar pressure, compared to the QMF buffer, the NB buffer, and the HM buffer, at the same two pressures. For each buffer, the upper (more oxidizing) curve is for the 4 kbar pressure. The calculated positions of the adjusted buffer systems for the three granitic rocks (Elberton, Stumpy Point, and Dinkey Dome) and for the three pelitic rocks (northern Idaho, south-central Maine, and southwestern Massachusetts) are shown. Arrow attached to each of the calculated regions indicates that the actual buffer condition for the rock may be more oxidizing (up-pointing arrow) or more reducing (downpointing arrow) because of the nature of the mineral assemblages. The only uncertainties shown are those related to the equilibrium temperatures except for the Maine sample, for which the uncertainty due to uncertainty in pressure is indicated for each of the two bounding temperature values.

Similarly, the excess Al in the octahedral site is assumed to affect the activity of annite only by decreasing the mole fraction of iron on that site; thus its effect is included by defining $X^{bt}_{Fe^{2+}}$ in equation (1) as the number of Fe^{2+} atoms/3.

In this paper, I do not consider the effect of K deficiency in biotite (Holdaway, 1980; Zen, 1981) on the activity of annite. The effect of F–OH substitution can be handled by the model of Hewitt and Wones, as expressed in equation (1).

For muscovite, I assumed that the octahedral aluminum is evenly distributed over the two equivalent sites, and an ideal mixing model is applied when other components enter that site, analogous to the model used for biotite, so that $\Delta G = -2RT \ln X^{mu}_{Al}$ where X^{mu}_{Al} is half of the number of atoms of octahedral Al in muscovite. For granitic rocks, the muscovite that shows textural evidence of being magmatic is usually celadonitic and X_{Al} is about 0.8–0.9 (Miller et al., 1981; Hammarstrom, 1982). For muscovite of metamorphic origin, the compositional correction is comparable or smaller. A small correction for the excess Si in tetrahedral sites can be made; just as for biotite, $\Delta \ln fo_2 = 4 \ln X^{mu}_{Si} = 4 \ln (4 - Y)/3$, where y = actual number of tetrahedral Al.

For both biotite and muscovite, another uncertainty that could affect the location of the reference BAMM buffer curve is order–disorder of tetrahedral Al and Si, the effect can be significant because the entropy of complete and ideal order–disorder of these atoms is 18.70 $JM^{-1}K^{-1}$ per 11 oxygen-formula of either mineral. The Gibbs free energy and entropy values of muscovite tabulated by Robie et al. (1978) are for crystals having total

tetrahedral disorder among the Si and Al atoms, but the entropy value of annite tabulated by Helgeson et al. (1978) are for crystals having total tetrahedral order among these atoms. If the tetrahedral atoms of muscovite are in fact ordered, the effect on the location of the reference BAMM curve will be to shift it by 18.70/2.303R = 0.98 log fO_2 units toward a more oxidizing position (Table 2, compare curves A and C or B and D). If, on the other hand, the tetrahedral atoms of annite are disordered, the effect on the location of the reference BAMM curve will be relatively minor (Table 2, curves C and D). The reason for this difference in effect is that the Gibbs free energy of annite was calculated from equation (3), using high temperature phase equilibrium data, and then extrapolated to 298 K, 1 bar using the entropy of annite. But in calculating the BAMM buffer for the temperature range shown in Figure 1, the same temperature-dependent entropy values were used, and so a large part of the effect of change of entropy of annite occasioned by the tetrahedral order–disorder was cancelled out; this cancellation is exact, for 1 bar pressure, at 787.7 K. The slope of the buffer curve for disordered annite is slightly steeper than the slope for ordered annite. In the temperature range of Figure 1, tetrahedral order–disorder in annite has a notable effect on the reference BAMM buffer curve only at temperatures higher than about 900 K, amounting to about 0.2 units in log fO_2 at 1000 K, the curve for disordered annite being more oxidizing. The parameters for the least-squares fitted equations for the four curves are given in Table 2.

For garnet, the principal components of solid solution with almandine are spessartine, $Mn_3Al_2Si_3O_{12}$, pyrope, $Mg_3Al_2Si_3O_{12}$, and grossular, $Ca_3Al_2Si_3O_{12}$. The ideal-solution model indicates a correction amounting to $+ 3RT \ln X^{gt}_{Fe^{2+}}$ where $X^{gt}_{Fe^{2+}}$ is the mole fraction of ferrous iron in garnet, i.e., $Fe^{2+}/3$. Cressey (1981) proposed that the almandine–grossular solid solution is nonideal, but the nonideal term is small for mole fraction of grossular less than 0.2. At a mole fraction value of grossular of 0.3, Cressey's data indicate that the excess entropy term contributes about 4.2 $JM^{-1}K^{-1}$ or about 0.2 units in log fO_2, enhancing the stability of the biotite–garnet side of the BAMM reaction. Following Saxena and Eriksson (1983), I assume that the Mg–Fe solid solution is ideal. Because most garnets in peraluminous rocks are low in the grossular component, in the applications to follow the nonideal term will be found to be negligible.

Both magnetite and quartz are assumed to have their ideal end member compositions and require no correction; such corrections are readily added if justified. The BAMM buffer reaction, adjusted for compositional corrections, can be therefore given as:

$$\log fO_2 = 10.29 - 26284T^{-1} + 0.148(P - 1)T^{-1} - 4\log X^{bt}_{Si} - 3\log X^{bt}_{Fe^{2+}} - 3\log X^{gt}_{Fe^{2+}} + 2\log X^{mu}_{Al^{VI}} + 4\log X^{mu}_{Si} \pm (650/T + 1) \quad (6)$$

Table 2. Parameters for least-squares fitted equations for the reference BAMM buffer curve; $\log fO_2 = a + bT^{-1} + c(P - 1)T^{-1}$

Curve	A	B	C	D
Muscovite	Disordered	Ordered	Disordered	Ordered
Biotite	Ordered	Ordered	Disordered	Disordered
a	10.29	11.26	11.26	12.24
b	-26284	-26284	-27053	-27053
c	0.148	0.148	0.148	0.148

Errors

A precise definition of the errors in the BAMM buffer equation is difficult to make; however, reasonable estimates can be made. Neither Hewitt and Wones (1981) nor Partin et al. (1983) gave estimates of errors of their equation for the stability of annite or ferriannite. The error given by Wones et al. (1971) was ±0.05 units in log fO_2. If we take that estimate to be the error for the more recent data of Hewitt and his coworkers, we obtain a value of ±4.6° for the temperature of breakdown of stoichiometric annite at one bar of hydrogen fugacity. In turn, this leads to an error of ±550 joules for the Gibbs free energy of formation of annite at 298 K.

For sanidine, muscovite, and quartz, the 298 K, 1 bar error for the molar Gibbs free energy of formation from the elements are given by Robie et al. (1978). These errors are, for sanidine, ±3.4 kJ; for muscovite, ±3.3 kJ; for quartz, ±1.1 kJ. The high temperature errors are assumed to be the same. For magnetite, the error given by Robie et al. (1978), ±2 kJ per mole, was applied to the data of Anovitz and Haas given in Table 1; this is probably a conservative estimate. For almandine, Anovitz and Haas gave an estimated error of ±1.5 kJ per mole at 298 K, 1 bar.

The error on the entropy of annite is difficult to evaluate. Helgeson et al. (1978) gave 298 K, 1 bar entropy estimates as well as the constants for a heat-capacity equation, but did not explicitly state the errors. If a generous error of ±20 $JM^{-1}K^{-1}$ is assumed, the contribution, over a range of 500°C, would be 10 kJ. The error on the Gibbs free energy of formation is the root-mean-square value of the errors on sanidine, magnetite, the high temperature experimental data on annite, and the entropy of annite, and amounts to ±10.8 kJ per mole (halving the error on the entropy of annite would reduce the error on annite to ±6.4 kJ).

The error on the location of the reference BAMM buffer curve is conservatively obtained by the root-mean-square value of the cumulative errors for the phases in reaction (3), taking into account the stoichiometric coefficients of the reaction. This is a conservative estimate because many thermochemical errors for different phases cancel in a balanced reaction. If an error of ±10.8 kJ is used for annite, the error on the Gibbs free energy of the

BAMM reaction would be 12.5 kJ. The error on the $T\log f_{O_2}$ term would then be 12,500/2.303R or 650. At 1000 K, the error would be ± 0.65 units in $\log f_{O_2}$; at 700 K it would be ± 0.93 units. If the error for annite is taken to be ± 6.4 kJ, the corresponding error for $T\log f_{O_2}$ would be 470; at 1000 K the error would be ± 0.47 in $\log f_{O_2}$, and at 700 K it would be ± 0.67. Errors that result from the use of various approximate solution models are estimated to be no more than ± 1 unit in $\log f_{O_2}$. Overall, the location of the BAMM buffer curve is probably good to about 1 to 1.5 units in $\log f_{O_2}$. These are largely systematic errors, however, and should not affect the relative locations of the observed mineral assemblages in $T - \log f_{O_2}$ space. For actual geologic situations, determinative errors in mineral chemistry and uncertainties in the equilibrium temperature probably affect the $\log f_{O_2}$ value at least as much as do the thermochemical errors. For example, an uncertainty of 50°C at 1000 K would introduce an error in $\log f_{O_2}$ of 1.3 units; at 700 K, the same temperature uncertainty would result in half again as much error in $\log f_{O_2}$ because of the steeper slope of the BAMM buffer curve in $T - \log f_{O_2}$ space at lower temperatures. In contrast, a pressure uncertainty as great as 2 kbar, at 1000 K, would contribute less than 0.3 units in $\log f_{O_2}$.

Geological applications: examples

Some peraluminous granites contain all the BAMM buffer minerals, and many peraluminous granites contain quartz plus three of the other four BAMM minerals. The BAMM buffer assemblage is also common in medium-grade metamorphic schists and gneisses derived from sedimentary or igneous rocks. If either biotite or almandine is absent in the rock, the oxygen fugacity would have been at a value more oxidizing than the buffer value. If either muscovite or magnetite is absent, the oxygen fugacity value would have been more reducing than the buffer. A biotite-garnet bearing rock should not be stable with hematite.

In peraluminous granitic rocks, an alkali feldspar is always present. Addition of a potassium feldspar to the BAMM buffer assemblage would increase the number of phases by one without adding a new component, so the thermodynamic variance of the system would be decreased by one. In a $T - \log f_{O_2}$ diagram at constant pressure, the assemblage would therefore define a piercing point that represents the intersection of two buffer curves: The BAMM reaction and reaction (2) which is the breakdown of annite to magnetite and sanidine. A buffer point is hardly useful as a petrologic tool; however, the fact that in peraluminous granites alkali feldspar, biotite and garnet are all solid solutions indicates that the presence of the BAMM buffer assemblage plus alkali feldspar can still be useful because of the variance added by the Mg and Al components in biotite, the Mg, Mn and Ca components in garnet, and the albitic component in the alkali feldspar.

To illustrate the utility of the BAMM buffer system, I will discuss three granitic rocks and three metamorphic rocks. All the calculations refer to tetrahedrally ordered biotite and disordered muscovite, consistent with the thermochemical values of Table 1.

The first example is from the Elberton Granite of northeastern Georgia. The petrology and petrography of the Elberton Granite were described by Stormer et al. (1980). The granite is mostly a fine-grained, even-textured grey rock that contains plagioclase, perthitic alkali feldspar, biotite, ferrian-ilmenite, magnetite, quartz, and muscovite; it does not contain garnet. Stormer et al. (1980) estimated a final crystallization temperature of about 650°C at a total pressure of about 4 kbar. Baldasari (1981) determined the oxygen fugacity of the rock at the time of crystallization on the basis of the compositions of the coexisting iron and titanium oxide phases. He suggested a $\log f_{O_2}$ value of -13.3 and a temperature of 685°C. By estimating the ferric-ferrous iron ratios in the biotite in equilibrium with magnetite (Wones and Eugster, 1965; Wones, 1972), he further suggested a $\log f_{O_2}$ value of about -15.0 to -15.6 at 680°C.

Baldasari (1981, table 5) presented microprobe data on the biotite. For nine determinations, the biotite averaged 1.42 aluminum per 11 oxygen formula of which 0.22 are octahedral, and an atomic Fe/Mg (total iron) ratio of 1.70. At 958 K and 4 kbar, the reference BAMM buffer value is $\log f_{O_2} = -16.4$ (Fig. 1). The excess tetrahedral Al correction for biotite is $+0.12$, the annite activity correction is $+0.88$, so the adjusted BAMM buffer value is -15.4. If the temperature had been 650°C instead of 685°C, the reference BAMM buffer value would be -17.6 and the adjusted buffer value would be -16.6. Because the mineral assemblage indicates that the actual value must be more oxidizing than the buffer value, the data are consistent with Baldasari's estimate based on either the oxide phases or the biotite composition.

Speer (1981) described a granite from Stumpy Point in eastern North Carolina. The rock contains plagioclase, perthitic alkali feldspar, biotite, muscovite, garnet, quartz, and ilmenite. Speers estimated the condition of final crystallization of the granite as about 650–700°C under about 2 kbar of total pressure. The biotite has an Fe/Mg of 3.03; it is highly aluminous with about 1.87 Al per 11 oxygen, of which 0.56 is octahedral. The garnet has 0.8 mole fraction of almandine and the spessartine + grossular components total 0.095. The reference BAMM buffer value at 700°C and 2 kbar is $\log f_{O_2} = -16.4$. The excess tetrahedral Al correction for biotite is $+0.19$, the annite activity correction is $+0.84$, the tetrahedral Al correction for muscovite is $+.13$, and the almandine activity correction is $+0.3$, so the adjusted BAMM buffer value is -15.0. At 650°C the corresponding reference value would be -17.9, and the adjusted value would be -16.5. Because magnetite is absent but ilmenite is present, the actual oxygen fugacity value must have been more reducing than the BAMM buffer value. Wones and

Eugster's (1965) calibration of biotite composition places the rock at a position on the log $fO_2 - T$ plot more oxidizing than the position of the NB buffer; at 700°C and 2 kbar, this value is −16.2 (Fig. 1), so the results are consistent.

The compositions of the coexisting biotite and garnet allow another estimate of the equilibration temperature. The composition of the garnet and the amount of octahedral Al in the biotite permit direct use of Ferry and Spear's (1978) 2-kbar biotite–garnet geothermometer. This resulted in T = 920°C. The 1-bar biotite–garnet geothermometer of Thompson (1976) gives a temperature of 800°C. Speer (1981) indicated that this mineral pair may represent an earlier stage in the history of crystallization. Because of this problem, I retained Speer's estimated temperature of consolidation in my calculations. If, however, the higher temperatures based on biotite and garnet record an earlier history, we will have a means to estimate the value of fO_2 at the corresponding early stage. For 800°C, the adjusted BAMM buffer value is −12.7.

Guy (1980) studied several plutons of the Dinkey Creek intrusive series in the Sierra Nevada batholith. One of the plutons, at Dinkey Dome, has a mineral assemblage that contains plagioclase, perthitic alkali feldspar, garnet, biotite, quartz, magnetite, and muscovite (the muscovite, however, according to Guy may not be magmatic). The mineral assemblage thus indicates a value of oxygen fugacity during crystallization more reducing than, but possibly the same as, the BAMM buffer. The biotite has 1.62 Al per 11 oxygen, of which 0.33 are octahedral, and its Fe/Mg ratio is 3.27. The garnet has about 0.69 mole fraction of almandine, its Fe/Mg ratio is 12.9, and the spessartine component plus minor grossular component amount to 0.24 mole fraction. The muscovite has 1.83 octahedral Al and 2.91 Si per 11 oxygen. Guy (1980) estimated the temperature of final crystallization to be about 670–700°C using the biotite–garnet geothermometer of Goldman and Albee (1977), and a total pressure of about 2–3 kbar. The Ferry and Spear (1978) biotite–garnet geothermometer, not corrected for the relatively high content of Mn and Ca in the garnet, also yields a temperature of 700°C, so I adopted this temperature in my calculations. The reference BAMM buffer at 2.5 kilobars and 700°C is −16.3 in log fO_2 units. The excess tetrahedral Al in biotite requires a correction of +0.18, the annite activity correction is +0.76, and the almandine activity correction is +0.5. The octahedral Al correction for muscovite is −0.1 and the Si correction is −0.1, so the adjusted log fO_2 value is −15.1. At 670°C, the corresponding reference value would be −17.2 and the adjusted value would be −16.0.

Three applications of the BAMM buffer to metamorphic rocks follow next. The first example is from the Belt Supergroup of northern Idaho, described by Hietanen (1969). Sample no. 2096, in the kyanite–staurolite zone, is described as a staurolite–garnet–biotite–muscovite schist, and contains magnetite and quartz in addition. Hietanen (1969) estimated temperature of 500–600°C and pressure of about 4 kbar. The biotite has 1.69 aluminum per 11 oxygens, of which 0.48 are octahedral, and an Fe/Mg ratio (total iron) of 0.75. The garnet has 0.72 mole fraction of almandine, and the Fe/Mg ratio is 5.54; the spessartine, grossular and andradite components total 0.15 mole fraction. The muscovite has 1.73 octahedral Al and 3.09 Si per 11 oxygen. Application of the biotite–garnet geothermometer gives about 500°C (Thompson, 1976; Ferry and Spear, 1978). Using this temperature, I calculated a reference BAMM buffer value of −23.0. The excess tetrahedral Al in biotite requires a correction of +0.13; the annite activity correction is +1.46, the almandine activity correction is +0.4; the muscovite Si correction is +0.1 and the octahedral Al correction −0.1, for an adjusted log fO_2 value of −21.0. If the temperature was 600°C, the reference log fO_2 value would be −19.1 and the adjusted value would be −17.3.

The second example is the mineral assemblage from a Buchan-type metamorphic rock of south-central Maine, described by Osberg (1971). His sample number 3a contains biotite, garnet, muscovite, magnetite, quartz, as well as plagioclase, staurolite, cordierite, chlorite, and ilmenite. The biotite has 1.82 Al per 11 oxygens, of which 0.58 are octahedral. The Fe/Mg ratio of the biotite is 0.99. The garnet has 0.72 mole fraction of the almandine component and its atomic Fe/Mg ratio is 6.58. The mole fraction of the spessartine component is 0.19. Osberg did not give a chemical analysis for the muscovite, so I assumed it to be $KAl_3Si_3O_{12}H_2$. Application of the biotite–garnet geothermometer (Thompson, 1976; Ferry and Spear, 1978) yields a temperature of 520°C, which is slightly higher than Osberg's (1971) estimate of 500°C. Osberg estimated a total pressure of about 2 kbar. Ferry (1976) estimated 3.5 kbar for the same area; this value may be high because of the andalusite–staurolite association about a meter away in the same outcrop. However, if we use Ferry's pressure and the biotite–garnet temperature, the reference BAMM buffer value is log fO_2 = −22.2. To this value must be added +0.14 for the excess tetrahedral Al in biotite, +1.19 for the annite activity correction, and +0.4 for the almandine activity correction, for an adjusted log fO_2 value of −20.5. If we used a pressure of 2 kbar, the final value would be more negative by 0.3; if we used a temperature of 500°C, the final value would be more negative by another 0.6. Even so, the final value is no more negative than about −21.6, considerably more oxidizing than the value of −24 estimated by Osberg (1971) based on the compositions of coexisting ilmenite and magnetite. Osberg (1971) determined the compositions of the oxide phases by X-ray cell measurements; he found the results to "vary from sample to sample". A log fO_2 value of −24 would make the system more reducing than the QMF buffer at 500°C (Osberg's estimated temperature), and is improbable because of the mineral assemblage. Ferry (1976) estimated, for his sample number 25, a value of log fO_2 of −22.5 on the basis of

compositions of fluid present during metamorphism; as this sample is located about 4 km away from Osberg's outcrop, it is doubtful the values can be compared.

A third example is the pelitic rocks of southwestern Massachusetts, described by Zen (1981). A pair of samples will be compared. Sample 103-1 contains biotite, garnet, muscovite, quartz, as well as chlorite, chloritoid, plagioclase, and ilmenite, but without magnetite. The biotite has 1.75 Al per 11 oxygens, of which 0.40 are octahedral. Its Fe/Mg ratio (total iron) is 2.23. The garnet has Fe/Mg ratio of 15.3, the almandine mole fraction is 0.82, and mole fraction of the spessartine plus grossular components amounts to 0.12. The muscovite has 1.8 octahedral Al and 3.09 Si. The biotite–garnet geothermometer of either Ferry and Spear (1978) or Thompson (1976) yields a temperature of about 500°C. The mineral assemblage, plus the fact that it is just below the Barrovian staurolite isograd, and a few kilometers away from a staurolite–kyanite assemblage, suggest a pressure of 3–4 kbar. Using a pressure of 3.5 kbar and 500°C, I obtained for the reference BAMM buffer system a value of $\log f_{O_2} = -23.1$. The excess tetrahedral Al correction for biotite is +0.22; the annite activity correction is +0.76, the almandine activity correction is +0.3, and the muscovite Si correction is +0.1 and the octahedral Al correction is −0.1. The adjusted BAMM buffer value is accordingly $\log f_{O_2} = -21.8$. The mineral assemblage must be more reducing than this value because it contains ilmenite rather than magnetite.

The second sample, 102-1, is located about 0.7 km to the southwest of 103-1, in the direction of decreasing metamorphic grade (Zen, 1981). The mineral assemblage is biotite, garnet, muscovite, magnetite, quartz, as well as pargasitic amphibole, chlorite, and plagioclase. This rock therefore contains all the BAMM minerals. The biotite has 1.67 Al per 11 oxygens, of which 0.32 are octahedral. Its Fe/Mg ratio is 1.48 (total iron). The garnet has Fe/Mg ratio of 12.1 and the almandine mole fraction is 0.64. The spessartine + grossular components account for 0.3 mole fraction, of which 0.2 is due to grossular. The muscovite has 1.84 octahedral Al and 3.05 Si per 11 oxygens. The high Ca and Mn contents suggest that the Ferry–Spear geothermometer may be only marginally serviceable (Ferry and Spear, 1978), but if applied leads to a temperature of 460°C, which is some 40°C cooler than for sample 103-1. Using this value of temperature and a pressure of 3.5 kilobars, I got for the reference BAMM buffer a value of $\log f_{O_2} = -24.9$. The excess tetrahedral Al correction for biotite is +0.22, the annite activity correction is +0.92, the almandine activity correction is +0.6, and the muscovite octahedral Al correction is −0.1 and the Si correction is +0.1. The adjusted $\log f_{O_2}$ value is therefore −23.2. This value is more negative than for sample 103-1, but the assemblage is more oxidizing because of the temperature difference.

Because temperatures of formation of rocks can rarely be determined to better than ±50°C, an intrinsic uncertainty exists in the estimated $\log f_{O_2}$ of about 1.3 unit for peraluminous granitic rocks (T in the range of 600°-700°C), and of about 2 units for medium-grade metamorphic rocks (T in the range of 350°-550°C). Even so, the BAMM assemblage appears to be useful to monitor and record the oxygen fugacity of many peraluminous rocks, particularly to compare the *relative* redox states of rocks in the same area. This is so because, consistent with the solid solution models adopted, the redox state recorded by the actual BAMM mineral assemblage is directly measured by the last four terms of equation (6). Even without data on the mineral chemistry, however, the presence of the entire buffer assemblage furnishes reasonable evidence that the oxygen fugacity value was intermediate between the NB and the HM buffers, in an area of the P–T–$\log f_{O_2}$ space for which few reference buffers now exist for peraluminous rocks.

Acknowledgments

This manuscript was critically reviewed by Richard N. Abbott, Jr., Robert A. Ayuso, David A. Hewitt, Theodore C. Labotka, Gilpin R. Robinson, Jr., John C. Stormer, Jr. and Priestley Toulmin, III. For their remarks that greatly improved the paper, I am much indebted. Larry Anovitz and John L. Haas, Jr., kindly let me use their unpublished thermochemical data on almandine and on magnetite, and Hewitt kindly let me use his unpublished experimental data and fitted equations on annite stability. I am grateful for these acts of generosity. Discussions with Jane Hammarstrom, Tren Haselton, and Pete Toulmin have been helpful to my understanding of peraluminous granites, and I thank them.

References

Baldasari, Arthur (1981) Iron–titanium oxides in the Elberton Granite. M.Sc. Thesis, University of Georgia, Athens.

Cressey, G. (1981) Entropies and enthalpies of aluminosilicate garnets. Contributions to Mineralogy and Petrology, 76, 413–419.

Czamanske, G. K. and Wones, D. R. (1973) Oxidation during magmatic differentiation, Finnmarka Complex, Oslo area, Norway, Part II: The mafic silicates. Journal of Petrology, 14, 349–380.

Ferry, J. M. (1976) P, T, fCO_2, and fH_2O during metamorphism of calcareous sediments in the Waterville-Vassalboro area, south-central Maine. Contributions to Mineralogy and Petrology, 57, 119–143.

Ferry, J. M. and Spear, F. S. (1978) Experimental calibration of the partitioning of Fe and Mg between biotite and garnet. Contributions to Mineralogy and Petrology, 66, 113–117.

Goldman, D. S. and Albee, A. L. (1977) Correlation of Mg/Fe partitioning between garnet and biotite with $^{18}O/^{16}O$ partitioning between quartz and magnetite. American Journal of Science, 277, 750–767.

Guy, R. E. (1980) The Dinkey Creek intrusive series, Huntington Lake quadrangle, Fresno County, California. M.Sc. Thesis, Virginia Polytechnic Institute and State University, Blacksburg.

Hammarstrom, J. M. (1982) Chemical and mineralogical variation in the Pioneer batholith, southwest Montana. U.S. Geological Survey Open-File Report 82-148.

Helgeson, H. C., Delany, J. M., Nesbitt, H. W., and Bird, D. K. (1978) Summary and critique of the thermodynamic properties of rock-forming minerals. American Journal of Science, 278-A.

Hewitt, D. A. (1978) A redetermination of the fayalite-magnetite-quartz equilibrium between 650° and 850°C. American Journal of Science, 278, 715–724.

Hewitt, D. A. and Wones, D. R. (1981) The annite-sanidine-magnetite equilibrium. Geological Association of Canada/Mineralogical Association of Canada/Canadian Geophysical Union Annual Meeting, Abstracts, 6, A-66.

Hietanen, Anna (1969) Distribution of Fe and Mg between garnet, staurolite, and biotite in aluminum-rich schist in various metamorphic zones north of the Idaho batholith. American Journal of Science, 267, 422–456.

Holdaway, M. J. (1980) Chemical formulae and activity models for biotite, muscovite, and chlorite applicable to pelitic metamorphic rocks. American Mineralogist, 65, 711–719.

Huebner, J. S. (1971) Buffering techniques for hydrostatic systems at elevated pressures. In G. C. Ulmer, Ed., Research techniques for high pressure and high temperature, p. 123–177. Springer-Verlag, New York.

Miller, C. F., Stoddard, E. F., Bradfish, L. J., and Dollase, W. A. (1981) Composition of plutonic muscovite: Genetic implications. Canadian Mineralogist, 19, 25–34.

Mueller, R. F. (1972) Stability of biotites: A discussion. American Mineralogist, 57, 300–316.

Osberg, P. H. (1971) An equilibrium model for Buchan-type metamorphic rocks, south-central Maine. American Mineralogist, 56, 570–586.

Partin, Elizabeth, Hewitt, D. A., and Wones, D. R. (1983) Quantification of ferric iron in biotite. Geological Society of America Abstracts with Programs, 15, 659.

Robie, R. A., Bethke, P. M., and Beardsley, K. M. (1967) Selected X-ray crystallographic data, molar volumes, and densities of minerals and related substances. U.S. Geological Survey Bulletin 1248.

Robie, R. A., Hemingway, B. S., and Fisher, J. R. (1978) Thermodynamic properties of minerals and related substances at 298.15K and 1 bar (10^5 pascals) pressure and at higher temperatures. U.S. Geological Survey Bulletin 1452.

Robinson, G. R., Jr., and Haas, J. L., Jr. (1983) Heat capacity, relative enthalpy, and calorimetric entropy of silicate minerals: An empirical method of prediction. American Mineralogist, 68, 541–553.

Saxena, S. K. and Eriksson, G. (1983) High temperature phase equilibria in a solar-composition gas. Geochimica et Cosmochimica Acta, 47, 1865–1874.

Schwab, R. G. and Küstner, D. (1981) Die Gleichgewichtsfugazitäten technologisch und petrologisch wichtiger Sauerstoffpuffer. Neues Jahrbuch für Mineralogie, Abhandlungen, 140, 111–142.

Speer, J. A. (1981) Petrology of cordierite- and almandine-bearing granitoid plutons of the southern Appalachian piedmont, U.S.A. Canadian Mineralogist, 19, 35–46.

Stormer, J. C., Jr., Whitney, J. A., and Hess, J. R. (1980) Petrology and geochemistry of the Elberton Granite: In J. C. Stormer, Jr. and J. A. Whitney, Eds., Geological, Geochemical, and Geophysical Studies of the Elberton Batholith, Eastern Georgia, p. 10–30. Georgia Department of Natural Resources, Environmental Protection Division, Georgia Geological Survey Guidebook 19.

Thompson, A. B. (1976) Mineral reactions in pelitic rocks: II. Calculation of some P–T–X(Fe–Mg) phase relations. American Journal of Science, 276, 425–454.

Wones, D. R. (1966) Mineralogical indicators of relative oxidation states of magmatic systems, (abstr.) American Geophysical Union, Transactions, 47, 216.

Wones, D. R. (1972) Stability of biotite: A reply. American Mineralogist, 57, 316–317.

Wones, D. R. (1981) Mafic minerals as indicators of intensive variables in granitic magmas. Mining Geology (Japan), 31, no. 4, 191–212.

Wones, D. R., Burns, R. G., and Carroll, B. M. (1971) Stability and properties of synthetic annite. (abstr.) EOS (American Geophysical Union Transactions), 52, 369–370.

Wones, D. R. and Eugster, H. P. (1965) Stability of biotite: Experiment, theory, and application. American Mineralogist, 50, 1228–1272.

Zen, E-an (1973) Thermochemical parameters of minerals from oxygen-buffered hydrothermal equilibrium data. Method, application to annite and almandine. Contributions to Mineralogy and Petrology, 39, 65–80.

Zen, E-an (1981) Metamorphic mineral assemblages of slightly calcic pelitic rocks in and around the Taconic allochthon, southwestern Massachusetts and adjacent Connecticut and New York. U.S. Geological Survey Professional Paper 1113.

Manuscript received, September 14, 1983;
accepted for publication, September 19, 1984.